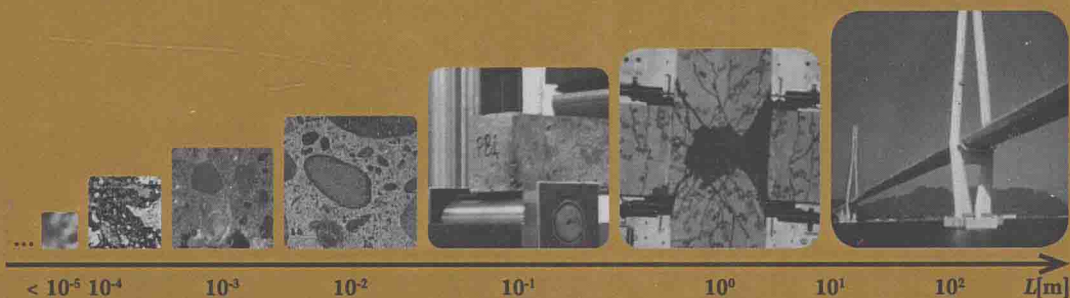


Computational Modelling of **CONCRETE STRUCTURES**

Editors:

*Nenad Bićanić, Herbert Mang
Günther Meschke, René de Borst*

Volume I



Computational Modelling of Concrete Structures

Editors

Nenad Bićanić

University of Rijeka, Croatia

University of Glasgow, Scotland, UK

Herbert Mang

Vienna University of Technology, Austria

Günther Meschke

Ruhr University Bochum, Germany

René de Borst

University of Glasgow, Scotland, UK

VOLUME 1



CRC Press

Taylor & Francis Group

Boca Raton London New York Leiden

CRC Press is an imprint of the
Taylor & Francis Group, an **informa** business

A BALKEMA BOOK

CRC Press/Balkema is an imprint of the Taylor & Francis Group, an informa business

© 2014 Taylor & Francis Group, London, UK

Typeset by V Publishing Solutions Pvt Ltd., Chennai, India

Printed and bound in Great Britain by CPI Group (UK) Ltd, Croydon, CR0 4YY

All rights reserved. No part of this publication or the information contained herein may be reproduced, stored in a retrieval system, or transmitted in any form or by any means, electronic, mechanical, by photocopying, recording or otherwise, without written prior permission from the publisher.

Although all care is taken to ensure integrity and the quality of this publication and the information herein, no responsibility is assumed by the publishers nor the author for any damage to the property or persons as a result of operation or use of this publication and/or the information contained herein.

Published by: CRC Press/Balkema

P.O. Box 11320, 2301 EH Leiden, The Netherlands

e-mail: Pub.NL@taylorandfrancis.com

www.crcpress.com – www.taylorandfrancis.com

ISBN: 978-1-138-00145-9 (set of two volumes)

ISBN: 978-1-138-02641-4 (Vol 1)

ISBN: 978-1-138-02642-1 (Vol 2)

ISBN: 978-1-315-76203-6 (eBook PDF)

Foreword

We kept our promise from four years ago and the EURO-C conference series reconvened again this spring in Austria, in St Anton am Alberg, from the 24th to 27th March 2014. This time, the proceedings comprise 6 invited and 107 contributed papers presented at the conference, keeping its tradition in line with predecessor conferences in the series (Innsbruck 1994, Badgastein 1998, St Johann im Pongau 2003, Mayrhofen 2006, Schladming 2010). Many participants will recall that the EURO-C series emerged as our joint undertaking following an increase in computational mechanics research of concrete generated at the time by the ICC 1984 conference held in Split, Croatia, the SCI-C 1990 conference in Zell am See, Austria and the two Concrete Mechanics Colloquia, held in Delft, The Netherlands in 1981 and 1987.

We express our sincere gratitude to the members (many of them long time regulars) of the International Advisory Panel (Zdenek Bažant, Sarah Billington, Alberto Carpinteri, Guillero Etse, Dariusz Gawin, Günther Hofstetter, Tony Jefferson, Milan Jirásek, Ragnar Larsson, Koichi Maekawa, Jacky Mazars, Javier Oliver, Jerzy Pamin, Gilles Pijaudier-Cabot, Marco di Prisco, Ekkehard Ramm, Jan Rots, Franz-Josef Ulm, Kaspar Willam and Yong Yuan) for their unwavering support and considerable effort in reviewing more than 160 abstracts. EURO-C conference series prides itself with a very rigorous reviewing process, aimed at safeguarding its tradition of scientific excellence, with high level quality of presented papers. The EURO-C series was fortunate to have witnessed many significant research breakthroughs and landmark papers over its long history and we trust that this high reputation will continue well into the future.

Conference papers are grouped into four distinct sections – (A) *Constitutive and Multiscale Modelling of Concrete* (B) *Advanced modelling strategies and paradigms* (C) *Time Dependent and Multiphysics Problems* (D) *Performance of concrete structures*.

We also strongly believe that the EURO-C 2014 Conference proceedings will again fulfil the role which the proceedings from the earlier EURO-C conferences undoubtedly enjoyed – to act as a valued and respected referential source for an up-to-date account of the current scientific debate on the research issues and advances in computational modelling of concrete and concrete structures, as well as on their relevance to the solution of complex problems in structural engineering practice.

Nenad Bićanić
Herbert Mang
Günther Meschke
René de Borst
Rijeka, Vienna, Bochum, Glasgow
January 2014

Table of contents

Foreword	xiii
VOLUME 1	
<i>Plenary lectures</i>	
Comminution of concrete due to kinetic energy of high shear strain rate <i>Z.P. Bažant & F.C. Caner</i>	3
Modeling failure of brittle materials with eigenerosion <i>A. Pandolfi, B. Li & M. Ortiz</i>	9
Multiscale computational models for the simulation of concrete materials and structures <i>G. Cusatis, R. Rezakhanlou, M. Alnaggar, X. Zhou & D. Pelessone</i>	23
Multi-scale (FE ²) analysis of material failure in cement/aggregate-type composite structures <i>J. Oliver, M. Caicedo, E. Roubin, J.A. Hernández & A. Huespe</i>	39
The aim of computational methods for managing concrete structures in nuclear power plants <i>E. Gdoutos, S. Michel-Ponnelle, J. Salin, G. Moreau, J. Sanahuja & C. Toulemonde</i>	51
Poro-chemo-fracture-mechanics ... bottom-up: Application to risk of fracture design of oil and gas cement sheath at early ages <i>F.-J. Ulm, M. Abuhaikal, T. Petersen & R.J.-M. Pellenq</i>	61
<i>Constitutive and multiscale modelling of concrete</i>	
Hierarchical multiscale models for localization phenomena within the framework of FE ² -X ¹ <i>J.F. Unger</i>	75
Modeling of Alkali-Silica Reaction in concrete: A multiscale approach for structural analysis <i>R. Esposito & M.A.N. Hendriks</i>	87
A novel strain-rate model for concrete and its influence on wave propagation due to impact <i>U. Häussler-Combe</i>	97
Implication of pore structure on micro-mechanical behaviour of virtual cementitious materials <i>N.L.B. Le, L.J. Sluys, M. Stroeve & P. Stroeve</i>	109
A constitutive model for concrete based on continuum theory with non-local softening coupled with eXtended Finite Element Method <i>J. Bobiński & J. Tejchman</i>	117
An elasto-plastic constitutive model with non-local softening and viscosity to describe dynamic concrete behaviour <i>I. Marzec & J. Tejchman</i>	127
Modelling cement at fundamental scales: From atoms to engineering strength and durability <i>E. Masoero, H.M. Jennings, F.-J. Ulm, E.D. Gado, H. Manzano, R.J.-M. Pellenq & S. Yip</i>	139
Two-scale model for concrete beams subjected to three point bending—numerical analyses and experiments <i>Ł. Skarżyński, M. Nitka & J. Tejchman</i>	149

A multiscale model for predicting the elasticity modulus and the strength of Ultra-High Performance Fiber Reinforced Concrete <i>J.L. Zhang, X. Liu, Y. Yuan & H.A. Mang</i>	159
Is cement a glassy material? <i>M. Bauchy, M.J.A. Qomi, R.J.-M. Pellenq & F.-J. Ulm</i>	169
Multi-scale model of a single crack bridge in composites combining rigid brittle matrix with heterogeneous fibrous reinforcement <i>M. Vořechovský, R. Rypel & R. Chudoba</i>	177
Modeling concrete under high frequency loading using a multi-scale method <i>A. Karamnejad, L.J. Sluys & V.P. Nguyen</i>	189
Mesoscopic modeling of triaxial behavior of concrete <i>Y. Malecot, L. Zingg, E. Piotrowska, M. Briffaut & L. Daudeville</i>	199
Application of a nonlocal damage law to model concrete fracture <i>E. Lorentz & K. Kazymyrenko</i>	209
An approach to modelling smoothed crack closure and aggregate interlock in the finite element analysis of concrete structures <i>A.D. Jefferson, I.C. Mihai & P. Lyons</i>	219
Modelling of fracture in three dimensional brittle bodies <i>Ł. Kaczmarezyk & C. Pearce</i>	225
Consideration of fibre orientation in a micromechanical model for strain hardening cement composite <i>I. Viejo, M. Lasपालas, I. Mariner & M.A. Jiménez</i>	237
Constitutive modelling of fibre reinforced cementitious composites based on micromechanics <i>I.C. Mihai, A.D. Jefferson & P. Lyons</i>	247
Non-local model and global-local cracking analysis for the study of size effect <i>C. Giry, C. Oliver-Leblond, F. Ragueneau & E. Kishta</i>	255
Numerical analysis of Recycled Aggregate Concrete mechanical behavior <i>P. Folino</i>	263
On finite element modeling of compressive failure in brittle materials <i>J. Červenka, V. Červenka & S. Laserna</i>	273
Influence of the macro-porosity and the meso-structure on the dynamic properties of concrete <i>F. Gatuingt & S. Pierre</i>	283
A volumetric upgrade of scalar gradient damage model <i>J. Pamin, A. Wosatko & R. Desmorat</i>	289
Nano-scale characterization of elastic properties of AFt and AFm phases of hydrated cement paste <i>S. Hajilar & B. Shafei</i>	299
ITZ-induced crack initiation in concrete: Micromechanics-based sensitivity analyses regarding concrete phase properties <i>M. Königsberger, B. Pichler & C. Hellmich</i>	307
Experimental and numerical investigation of the mechanical behavior of interfaces between cementitious materials <i>T. Cordes & G. Hofstetter</i>	319
A continuum micromechanics-LEFM model for fiber reinforced concrete <i>J.J. Timothy & G. Meschke</i>	327

Advanced modelling strategies and paradigms

Compressive behavior of a lattice discrete element model for quasi-brittle materials <i>M. Vassaux, F. Ragueneau, B. Richard & A. Millard</i>	335
Discrete modeling of micro-structure evolution during concrete fracture using DEM <i>M. Nitka & J. Teichman</i>	345
Numerical simulations of the bond between concrete and perforated metal sheets within composite slabs <i>S. Pirringer & J. Kollegger</i>	355
Lattice discrete particle modeling of buckling deformation in thin ultra-high-performance fiber-reinforced concrete plates <i>R.G. El-Helou, C.D. Moen, E. Lale & G. Cusatis</i>	365
Numerical analysis of linear viscoelastic 3D concrete specimens: Comparison between FE and FFT methods <i>B. Bary, L. Gélébart, E. Adam & C. Bourcier</i>	373
Modeling of multiple cracks in reinforced concrete members using solid finite elements with high aspect ratio <i>O.L. Manzoli, M.A. Maedo, E.A. Rodrigues & T.N. Bittencourt</i>	383
Correlations in the mesoscale modelling of fracture of quasi-brittle materials – extracting internal lengths <i>V. Lefort, G. Pijaudier-Cabot, D. Grégoire & P. Grassl</i>	393
Computing permeation properties of mortar from pore size distributions <i>F. Khaddour, D. Grégoire & G. Pijaudier-Cabot</i>	405
Prediction of cracks in concrete due to strain incompatibilities at the mesoscopic scale <i>F. Benboudjema, C. De Sa & F. Lagier</i>	415
Statistical distribution and size effect of residual strength after a period of sustained load <i>M. Salviato, K. Kirane & Z.P. Bažant</i>	423
A constrained Large Time INcrement algorithm for quasi-brittle fracture: Implementation and optimisation aspects <i>B. Vandoren, A. Simone & L.J. Sluys</i>	429
Localization analysis of coupled plasticity and damage models for dissipative materials <i>G. Xotta, S. Bezae & K.J. Willam</i>	439
Numerical modeling support for form-finding and manufacturing of folded plate structures made of cementitious composites using origami principles <i>R. Chudoba, J. van der Woerd & J. Hegger</i>	451
Numerical modelling of cracking in Steel Fibre Reinforced Concretes (SFRC) structures <i>J.-L. Tailhan, P. Rossi & D. Daviau-Desnoyers</i>	463
A new method for calculating local response in elastic media—the embedded unit cell approach <i>M. Grigorovitch & E. Gal</i>	471
Lattice models of debonding in composite concrete pavements <i>D. Tompkins, L. Khazanovich & J.E. Bolander</i>	477
Parametric FE studies on a coupled energetic-statistical size effect in plain concrete beams under bending <i>E. Syroka-Korol & J. Teichman</i>	487
Elastic-brittle fraction model for concrete and masonry structures <i>M.A.N. Hendriks & J.G. Rots</i>	495

A numerical approach for the evaluation of the structural redistribution coefficient K_{rel} <i>M. di Prisco & P. Martinelli</i>	503
Comparison of nonlocal and crack-band damage-plasticity approaches for modelling the failure of reinforced concrete structures <i>D. Xenos & P. Grassl</i>	513
Adaptive strain path-following control for softening material <i>T. Pohl, M. Bischoff & E. Ramm</i>	521
3D cohesive crack propagation using hybrid-Trefftz finite elements <i>C.J. Pearce, G. Edwards & L. Kaczmarczyk</i>	531
Zero-thickness interface model for coupled thermo-mechanical failure analysis of concrete <i>A. Caggiano & G. Etse</i>	541
Using XFEM for modelling localized fracture of reinforced concrete beams <i>F.Y. Liao & Z. Huang</i>	551
Development of full-scale finite-element models to evaluate corroding concrete slabs <i>B. Shafei & A. Alipour</i>	561
Modelling cracking in reinforced-concrete beams using beam finite elements with embedded discontinuity <i>P. Ščulac & G. Jelenić</i>	569
Numerical modeling of steel Fiber Reinforced Concrete on the meso- and macro-scale <i>Y. Zhan, H.G. Bui, J. Ninic, S.A. Mohseni & G. Meschke</i>	579
Author index	587

VOLUME 2

Time dependent and multiphysics problems

Reorientation of fibres during the flow of fibre-reinforced self-compacting concrete and determination of fibre orientation factor <i>S. Kulasegaram, R. Deeb & B.L. Karihaloo</i>	593
Fire resistance analysis of RC elements with restrained thermal elongation in a natural fire <i>A. Sadaoui, A. Khennane & M. Fafard</i>	603
Accounting for the fibre orientation on the structural performance of flowable fibre reinforced concrete <i>E.V. Sarmiento, M.A.N. Hendriks & T. Kanstad</i>	609
Analysis of the thermo-chemo-mechanical behavior of massive concrete structures at early-age <i>T. Honorio, B. Bary & F. Benboudjema</i>	619
Modeling the rapid chloride migration test for concrete using the lattice model and characteristic Galerkin approach <i>B. Šavija, M. Luković & E. Schlangen</i>	629
Diffusion-reaction model for ASR: Formulation and 1D numerical implementation <i>J. Liaudat, C.M. López & I. Carol</i>	639
A coupled carbonation-rust formation-mechanical damage model for steel corrosion in reinforced concrete <i>T.T.H. Nguyen, B. Bary, T. DeLarrard & V. L'Hostis</i>	649
Drying cracking pattern analysis using a simple two-stage drying model and a discrete model <i>A. Delaplace & H. Noyalet</i>	659

Microscopic model for concrete diffusivity prediction <i>M. Bogdan, F. Benboudjema, J.-B. Colliat & L. Stefan</i>	667
Model B4: Multi-decade creep and shrinkage prediction of traditional and modern concretes <i>R. Wendner, M.H. Hubler & Z.P. Bažant</i>	679
Concrete behaviour under ballistic impacts: Effects of materials parameters to penetration resistance and modeling with PRM model <i>C. Pontiroli, B. Erzar & E. Buzaud</i>	685
Modeling dynamic fracture of quasi-brittle materials: Rate sensitivity and impact <i>J. Ožbolt, B. Irhan, A. Sharma & D. Ruta</i>	695
Modeling processes related to corrosion of steel reinforcement and damage in concrete <i>J. Ožbolt, F. Oršanić & G. Balabanić</i>	705
Computational failure analysis of concrete under high temperature <i>G. Etse, M. Ripani & J.L. Mroginiski</i>	715
Thermal effects on early-age cracking potential of concrete bridge decks <i>J.E. Bolander, K. Kim & K. Sasaki</i>	723
The influence of loading rate on the compressive strength of cementitious materials: Experiments and “separation of time scales”-based analysis <i>B. Pichler, I. Fischer, E. Lach, Ch. Terner, E. Barraud & F. Britz</i>	731
A numerical model for the self-healing capacity of cementitious composites <i>G. Di Luzio, L. Ferrara & V. Krelani</i>	741
Microprestress-solidification theory: Modeling of size effect on drying creep <i>Z.P. Bažant, P. Havlásek & M. Jirásek</i>	749
A 2D hydro-mechanical lattice approach for modelling corrosion induced cracking of reinforced concrete <i>P. Grassl, C. Fahy, S. Wheeler & D. Gallipoli</i>	759
Chemoplastic modelling of Alkali-Silica Reaction (ASR) <i>A. Winnicki, S. Serega & F. Norys</i>	765
Three-dimensional network modelling of the influence of microstructure of concrete on water transport <i>I. Athanasiadis, S. Wheeler & P. Grassl</i>	775
Modelling of chloride transport in non-saturated concrete <i>M. Fenaux, J.C. Gálvez, E. Reyes, A. Moragues & J. Bernal</i>	781
Numerical analysis of multiple ion species diffusion and Alkali-Silica Reaction in concrete <i>M.N. Nguyen, J.J. Timothy & G. Meschke</i>	789
Multi-scales computation of creep deformation of concrete at very early-age <i>M. Farah, F. Grondin, A. Loukili & M. Matallah</i>	797
<i>Performance of concrete structures</i>	
Compressive membrane action in confined RC and SFRC circular slabs <i>B. Belletti, F. Vitulli & J.C. Walraven</i>	807
Influence of differential settlements on masonry structures <i>H. Nasser, M. Al Heib & O. Deck</i>	819
Numerical study of a strain hardening cementitious composite overlay system for durable concrete repair <i>M. Luković, E. Schlagen, B. Šavija, G. Ye & K. van Breugel</i>	827
Discussion on mechanical behavior of joints using post-installed anchors and concrete surface roughening for seismic retrofitting <i>Y. Takase, T. Abe, T. Ikeda, T. Wada, K. Katori & Y. Shinohara</i>	837

Assessing the structural behavior of shear-critical prestressed concrete beams using Finite Element analysis and digital image correlation <i>K. De Wilder, G. De Roeck, L. Vandewalle, P. Lava, Y. Wang & D. Debruyne</i>	847
Bending load capacity of strengthened RC beams with stochastically distributed material properties <i>J. Weselek & U. Häussler-Combe</i>	859
Study of brittle failure modes of precast roof elements connected to the beams with steel dowels <i>B. Belletti, C. Damoni, M. Scolari & A. Stocchi</i>	871
Non-linear analyses and cracking process of FRC tension ties <i>P. Bernardi, E. Michelini, A. Sirico, F. Minelli & G. Tiberti</i>	883
Non-linear mechanical analysis of shield tunnel structure at ultimate loading <i>H. Zhang, X. Liu & Y. Yuan</i>	893
Non-linear analysis of mechanical behaviors of shield tunnel segments reinforced by steel plate <i>M. Tang, X. Liu & Y. Yuan</i>	899
Crack tracking on a shear critical reinforced concrete beam <i>A.T. Slobbe, M.A.N. Hendriks & J.G. Rots</i>	905
Nonlinear FE analysis of a full scale in situ test on a RC bridge by means of a 1D layered frame model <i>D. Ferreira, J. Bairán & A. Mari</i>	917
Determination of distribution width for shear stresses at support in reinforced concrete slab bridges <i>E.O.L. Lantsoght, A. de Boer & C. van der Veen</i>	927
Numerical analysis for predicting the ultimate capacity of rectangular reinforced concrete stub columns <i>A.A. El Fattah & H. Rasheed</i>	937
Formulation for the adjustment of RC-section behaviour to experimental tests <i>A.T. López, A. Tomás & G. Sánchez-Olivares</i>	947
Modeling viscous damping in nonlinear direct-integration and modal time-history analyses of base-isolated reinforced concrete buildings <i>D.R. Pant & A.C. Wijeyewickrema</i>	957
Three-dimensional FE simulation of pullout test of corroded bar from RC specimen <i>M. German & J. Pamin</i>	967
Nonlinear FEA guideline for modelling of concrete infrastructure objects <i>A. de Boer, M.A.N. Hendriks, J.A. den Uijl, B. Belletti & C. Damoni</i>	977
Simplified method strategies based on damage mechanics for engineering issues <i>J. Mazars & S. Grange</i>	987
Numerical investigation of the bearing capacity of transversely prestressed concrete deck slabs <i>S. Amir, C. van der Veen, J.C. Walraven & A. de Boer</i>	999
Fatigue testing and numerical simulation of mono strand stay cable systems <i>J. Novoszel, W. Traeger & J. Kollegger</i>	1011
Pressure-impulse diagrams for SFRC underground tunnels <i>M. Colombo, P. Martinelli & R. Huaping</i>	1023
Safety assessment of a bridge deck slab using NLFEA and a semi-probabilistic global resistance safety factor <i>M. Pimentel & J. Figueiras</i>	1031

FEM and Strut-and-Tie analysis of RC frame corners under opening bending moment <i>M. Szczecina & A. Winnicki</i>	1041
Pavement infrastructures footprint: The impact of pavement properties on vehicle fuel consumption <i>A. Louhghalam, M. Akharian & F.-J. Ulm</i>	1051
Simulating bond-slip effects in high-performance fiber-reinforced cement based composites under cyclic loads <i>M.J. Bandelt & S.L. Billington</i>	1059
Simulation of large strains in concrete specimen—centric tensile tests using steel ropes as reinforcement <i>B. Kromoser, B. Eichwalder & J. Kollegger</i>	1067
Numerical simulation of shear behavior of reinforced concrete beams with and without flanges <i>P. Huber & J. Kollegger</i>	1073
Introduction of warping in a nonlinear multifiber beam model in torsion for reinforced concrete structures <i>S. Capdevielle, S. Grange, F. Dufour & C. Desprez</i>	1081
Author index	1089

Plenary lectures

Comminution of concrete due to kinetic energy of high shear strain rate

Z.P. Bažant

Department of Civil Engineering, Northwestern University, Evanston, Illinois, USA

F.C. Caner

Institute of Energy Technologies, School of Industrial Engineering, University Politecnica de Catalunya, Barcelona, Spain

ABSTRACT: This paper outlines the basic idea of a macroscopic model on the dynamic comminution or fragmentation of rocks, concrete, metals, and ceramics. The key idea is that the driving force of comminution under high-rate shear and compression with shear is the release of the local kinetic energy of shear strain rate. The spatial derivative of the energy dissipated by comminution gives a force resisting the penetration, which is superposed on the nodal forces obtained from the static constitutive model in a finite element program. The present theory is inspired partly by Grady's model for comminution due to explosion inside a hollow sphere, and partly by analogy with turbulence. In high velocity turbulent flow, the energy dissipation rate gets enhanced by the formation of micro-vortices (eddies) which dissipate energy by viscous shear stress. Similarly, here it is assumed that the energy dissipation at fast deformation of a confined solid gets enhanced by the release of kinetic energy of the motion associated with a high-rate shear strain of particles. For simplicity, the shape of these particles in the plane of maximum shear rate is considered to be regular space-filling hexagons. The particle sizes are considered to be distributed according to the Schuhmann power law, but the formulation for any other suitable distribution can easily be obtained by replacing the Schuhmann distribution by the desired distribution. The condition that the rate of release of the local kinetic energy must be equal to the interface fracture energy yields a relation between the particle size, the shear strain rate, the fracture energy and the mass density. The density of this energy at strain rates $>1,000/s$ is found to exceed the maximum possible strain energy density by orders of magnitude, making the strain energy irrelevant. It is shown that particle size is proportional to the $-2/3$ power of the shear strain rate and the $2/3$ power of the interface fracture energy or interface shear stress, and that the comminution process is macroscopically equivalent to an apparent shear viscosity that is proportional (at constant interface friction) to the $-1/3$ power of this rate. A dimensionless indicator of the comminution intensity is formulated. After comminution, the interface fracture energy takes the role of interface friction, and it is pointed out that if the friction depends on the slip rate, the aforementioned exponents would change. The effect of dynamic comminution can simply be taken into account by introducing the apparent viscosity into the material constitutive model. The theory was inspired by noting that the local kinetic energy of shear strain rate plays a role analogous to the local kinetic energy of eddies in turbulent flow.

1 INTRODUCTION

The previous studies of high-rate dynamic fracture of rocks, concretes, ceramics, composites and metals have dealt mainly with the nucleation, propagation and branching of a dynamically propagating crack, their interference with elastic or shock waves, and the mechanism of development of the zones of densely distributed fractures, called the Mescall zones (Mescall and Weiss 1984, Freund 1990, Doyoyo 2002, Deshpande and Evans 2008, Wei et al. 2009). However, a comminution model in the form of a macroscopic constitutive equation

that could be used in large dynamic finite element programs for global response of structures had been lacking until a fundamentally new kind of approach, based on the release of kinetic energy of shearing, was proposed in 2013 (Bažant and Caner 2013). The theory proposed here is partly inspired by analogy with turbulence. In high velocity turbulent flow, the rate at which energy is dissipated increased significantly by viscous shear stress. Similarly, energy dissipation in rapidly deforming confined solids must be enhanced by the release of the kinetic energy of high shear strain rate of fragmenting solid. Another inspiration for the

present model is Grady's model for explosion in a hollow sphere (Grady, 1982). In that model, the kinetic energy of volumetric strain is considered to cause comminution. Grady calculated and experimentally justified that the average particle size is given by $\bar{s} = (48\Gamma/\rho\dot{\epsilon}_p^2)^{1/3}$ where Γ = interface fracture energy, ρ = mass density and $\dot{\epsilon}_p$ = volumetric strain rate. However, application of this equation to impact was not justified theoretically. This paper reviews the new and rigorous theoretical justification of the energy dissipation caused by comminution and discusses its application to fracturing of concretes and rocks. Application to missile impact will appear in detail in Bažant and Caner (2013b).

2 THEORETICAL FORMULATION

2.1 Main assumptions and analogy with turbulence

We begin with the analysis of a simple idealized process in which the solid is comminuted to identical particles (Fig. 1). In the plane of maximum shear, we assume a regular hexagonal subdivision because it is space-filling and gives the smallest surface-to-volume ratio (Fig. 1a) and thus requires the minimum energy to form. In the direction normal to the hexagons, we assume the particles to be prismatic.

Consider that, at a certain moment, the strain rate (shown in Fig. 1b as a displacement regarded as infinitesimal) becomes high enough for the kinetic energy of shear strain rate to suffice for creating the fractures and interface slips that separate the particles of as yet unknown size. As that happens, the particles release their local kinetic energy, slip against each other, and regain their original undeformed shape after comminution, while the particle centers conform to the same macroscopic velocity field (Fig. 1c).

Assuming particle symmetry with respect to axes x and y , the simplified drop of kinetic energy

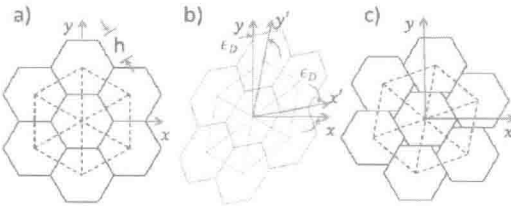


Figure 1. The comminution of material into prismatic hexagonal particles: (a) Undeformed material, (b) sheared material, and (c) comminuted material. The velocities are shown as infinitesimal displacements. The gaps at the hexagon corners are second-order small and thus negligible.

of the hexagonal prisms per unit volume due to comminution is:

$$\Delta K = -\frac{h}{V_p A} \int \frac{1}{2} (\dot{u}^2 + \dot{v}^2 - (\dot{u}^+)^2 - (\dot{v}^+)^2) dx dy = -c_k \rho h^2 \dot{\epsilon}_p^2 \quad (1)$$

where A = particle area, ρ = mass density, $c_k = I_p/(2hV_p)$, $V_p = (3\sqrt{3}/8)h^3$ = particle volume, and $I_p = (\sqrt{3}/32)h^4$ = polar moment of inertia of each hexagonal prism of side h . It is interesting that the kinetic energy K_{deur} of a particle deforming by pure shear at rate $\dot{\epsilon}_p$ happens to be the same as the kinetic energy K_{eddy} of an eddy rotating as a rigid body of the same size at angular rate $\dot{\omega} = \dot{\epsilon}_p$. In both comminution and turbulence, the micro-level kinetic energy augments the kinetic energy of the macro-level motion.

2.2 Comminuted particle size distribution

In this work, particle sizes are considered to vary randomly, according to the following cumulative distribution (Schuhmann 1940, Charles 1957, Cunningham 1987, Ouchterlony 2005):

$$F(s) = \frac{s^k - h^k}{H^k - h^k}; \quad h \leq s \leq H, \quad 0 \leq F(s) \leq 1 \quad (2)$$

where k = empirical constant ($k \approx 0.5$), s = variable particle size; and h , H = minimum and maximum particle sizes (usually $H/h = 10$ to 100). Since the macroscopic quasi-static constitutive law with non-localized strain softening includes the energy dissipation corresponding to material crushing into particles of the size d_a of the largest material inhomogeneities, H should be considered as one order of magnitude smaller, i.e., about $0.1 d_a$. Then, the combined interface area per unit volume can be expressed as $S = C/h$. The loss of kinetic energy of the shear strain rate of the particles of all sizes per unit volume is given by $\Delta K = -\int_{s=h}^H c_k \rho s^2 \dot{\epsilon}_p^2 dF(s) = -C_k \rho h^2 \dot{\epsilon}_p^2$ where \bar{c} , C_s and C_k are dimensionless constants.

Assuming that all of a kinetic energy decrement K is dissipated by an interface fracture energy increment $\Gamma \Delta S$, the interface fracture (or frictional slip) can occur when:

$$-\frac{\Delta K}{S} = -\frac{d\Delta K/dh}{dS/dh} = \Gamma \quad (3)$$

After substitutions into Eq. (3) one gets:

$$h = \left(\frac{C_s \Gamma}{\rho \dot{\epsilon}_p^2} \right)^{1/3} \quad (4)$$

where C_s is a dimensionless constant.

It is worth noting here that $h \propto \dot{\epsilon}_D^{2/3}$. This result is in agreement with what Grady (1998) verified empirically (though not theoretically) for the impact of missiles and it serves as one experimental verification of the present theory (Eq. 4).

2.3 Energy dissipation due to comminution and its implementation in a constitutive law

Substitution of Eq. (4) into (1) further yields:

$$\Delta K = -(C_0 \Gamma^2 \rho)^{1/3} \dot{\epsilon}_D^{2/3} \quad (5)$$

where C_0 is a certain dimensionless constant. This expression suggests how to implement the energy sink due to comminution in a constitutive law for a macroscopic structural analysis. Note that ΔK has the dimension of a stress and can be interpreted as such.

To obtain a three-dimensional generalization, it is convenient to introduce an equivalent viscosity η_D such that the viscous stress strain relation $s_{ij} = \eta_D \dot{\epsilon}_{Dij}$ would give the same energy dissipation density as Eq. (5) for any deviatoric strain rate tensor in the variational sense; here s_{ij} is the additional deviatoric stress caused by the comminution.

Since 1) the energy density is the same as the stress, 2) s_{12} must be equal to ΔK when all other tensorial components vanish and 3) ΔK must be a tensorial invariant, it is necessary that $-\Delta K = \sqrt{s_{ij}s_{ij}}/2$. Accordingly, the energy sink due to the comminution process may be modeled by the equivalent viscosity:

$$\eta_D = (C_0 \Gamma^2 \rho)^{1/3} \dot{\epsilon}_D^{-1/3} \quad (6)$$

where $\dot{\epsilon}_D = \sqrt{\dot{\epsilon}_{Dij}\dot{\epsilon}_{Dij}}/2$.

Viscosity η_D can easily be implemented in the constitutive relation in a finite element program. It may be noted that the enhancement of dissipative viscous resistance to shearing is again a feature analogous to the enhancement of viscous resistance to flow due to turbulent eddies.

Finite element simulations indicate that, in practical applications such as impact, the rate of expansive volumetric strain rate, $\dot{\epsilon}_V$, plays no significant role. For explosions in a shale rock or in confined concrete, though, both of the rates of shear strain and of volumetric expansion may be important. It can be shown that, in that case, the foregoing theory can easily be generalized; e.g., $\dot{\epsilon}_D^{-1/3}$ in Eq. (6) needs to be replaced by $(\dot{\epsilon}_D^2 + \dot{\epsilon}_V^2)^{-1/6}$.

2.4 The comminution intensity dimensionless indicator

In view of the partial analogy with turbulence we introduce a dimensionless indicator of

comminution intensity. The strain energy density U that is stored in the material may be expressed as $U = \tau^2/2G$ where G is the elastic shear modulus and τ is the shear stress. When $\Delta K \gg U$, then obviously the comminution cannot be caused by the release of strain energy and the release of kinetic energy is the only possible energy source for the comminution. Therefore, we may define the dimensionless number: $B_a = -\Delta K/U$ or:

$$B_a = \frac{G}{C_g \tau^2} (\Gamma^2 \rho \dot{\epsilon}_D^2)^{1/3} \quad (7)$$

which has the property that the comminution is:

$$\begin{aligned} &\text{kinetic energy driven if } B_a \gg 1, \\ &\text{in transition if } B_a \approx 1, \\ &\text{absent if } B_a \ll 1. \end{aligned} \quad (8)$$

The equivalent viscosity may also be uniquely expressed in terms of B_a .

2.5 Transition formulation and apparent viscosity

For small shear strain rates, Eq. (6) cannot be applied directly not only because as $\dot{\epsilon}_D \rightarrow 0$, $\eta_D \rightarrow \infty$, but also at small shear strain rates, comminution should cease to happen. To deduce the form of the transition formula, the viscosity given in Eq. (6) can be expressed in terms of B_a :

$$\eta_D = \frac{\Gamma}{\tau} \left(\frac{C_0^{2/3} G \rho}{C_g B_a} \right)^{1/2} \quad (9)$$

The transitional apparent viscosity must approach to zero for $B_a \ll 1$ and at the other extreme it should approach to Eq. (9) for $B_a \gg 1$. Thus the transitional apparent viscosity can be expressed as

$$\eta_D = \frac{\Gamma}{\tau} \left(\frac{C_0^{2/3} G \rho}{C_g} \frac{B_a^{n-1}}{1 + B_a^n} \right)^{1/2} \quad (10)$$

where n = an empirical constant controlling how sharp the transition is; $n \geq 1$.

3 RESULTS AND DISCUSSION

Comminution takes place in high speed perforation of concrete structures for which several data are available in the literature. One such data (Adley et al. 2012) is shown in Fig. (2), which shows as a function of the thickness of the wall. The entry velocity of the missile is 310 m/s. The values are computed with an explicit dynamic finite element

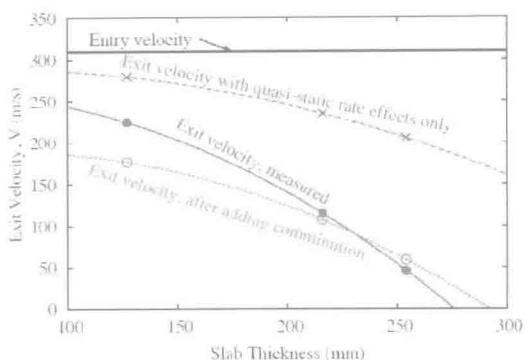


Figure 2. The comparison of measured exit velocities and predictions by model M7 using only quasi-static strain rate effect and both quasi-static strain rate effect and effect of comminution of concrete

program using the microplane model, first under the assumption that the only rate effects are the quasistatically calibrated rate effects, which consist of viscoelasticity of intact concrete between the cracks and of the rate of bond breakage at the fracture front controlled by activation energy (Bažant and Caner 2013, Caner and Bažant 2013). As seen, this simple assumption leads to a gross overestimation of the exit velocities. However, when the presently formulated equivalent viscosity due to kinetic comminution is included, the data for the two thicker walls are fitted perfectly.

For the thinnest wall, the exit velocity is still overestimated (Fig. 2). However, this is likely explained by differences in the specific moisture contents in the nanopores of concrete. For a lower moisture content, Hopkinson bar experiments have shown a lower strength in high-rate shear, and this is the case for the thinner wall since it dries faster.

In Fig. (3), the experimental and predicted crater shapes are shown. The predictions are for a projectile guided so that it impacts the wall at a right angle and exits the wall at a right angle too, because the experimental crater shapes were available only for that case, although in general the projectiles must be exiting at a different angle than the impact angle. Nevertheless, the predicted crater shapes are in good agreement with the experimental shapes for all three slabs. In obtaining these predicted crater shapes, elements distorted excessively have been eroded, and as the erosion criteria, a max. principle strain of 0.005 and 0.01 have been employed with little difference in the results but significantly longer runtimes when the larger threshold is used.

Another intriguing application of this dynamic comminution theory may be the fracturing of gas

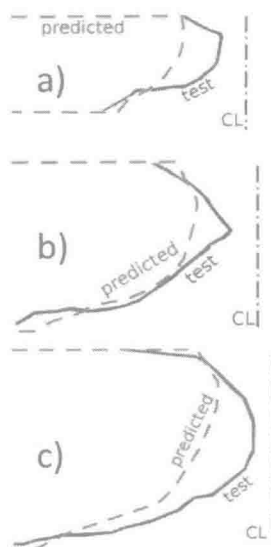


Figure 3. Experimental (solid lines) and predicted (dashed line) crater shapes in the perforation of a) 127 mm, b) 216 mm and c) 254 mm plain concrete walls.

or oil shale by electro-hydraulic pulsed arc (Maurel et al. 2010) or by chemical explosion in the pipe of a horizontal borehole. However, since no such data exist in the public domain, the application of the present comminution theory in fracture of shale rock is yet to be carried out.

4 CONCLUSIONS

In this paper, a macroscopic model on the dynamic comminution or fragmentation of rocks, concrete, metals, and ceramics is presented. The main assumption is that the driving force of comminution under high-rate compression is the release of the local kinetic energy of shear strain rate. The present theory indicates that the density of kinetic energy available for comminution is proportional to the $(2/3)$ power of the shear strain rate, the particle size or crack spacing is proportional and the $(-2/3)$ power of that rate, and the energy dissipation by comminution is equivalent to a shear viscosity decreasing as the $(-1/3)$ power of that rate. Confirmation of the theory is provided by fitting the data on both the measured exit velocity of projectiles penetrating concrete walls of different thicknesses and the measured crater shapes in these walls.

The formulation, in principle, can be applied to the fracturing of gas or oil shale by electro-hydraulic pulsed arc or by chemical explosion in the pipe of a horizontal borehole as well.